Journal of Power Sources 196 (2011) 847–850

Contents lists available at ScienceDirect

Journal of Power Sources

journal homepage: www.elsevier.com/locate/jpowsour

Short communication

A hierarchical nanostructure consisting of amorphous MnO_2, Mn_3O_4 nanocrystallites, and single-crystalline MnOOH nanowires for supercapacitors

Chi-Chang Hu[a,*], Ching-Yun Hung[a], Kuo-Hsin Chang[a,b], Yi-Lin Yang[b]

[a] Department of Chemical Engineering, National Tsing Hua University, Hsin-Chu 30013, Taiwan
[b] Department of Chemical Engineering, National Chung Cheng University, Chia-Yi 621, Taiwan

ARTICLE INFO

Article history:
Received 11 March 2010
Received in revised form 28 June 2010
Accepted 3 August 2010
Available online 7 August 2010

Keywords:
Ternary nanocomposite
Manganese oxides
Cycle stability
Supercapacitor

ABSTRACT

In this communication, a porous hierarchical nanostructure consisting of amorphous MnO_2 (a-MnO_2), Mn_3O_4 nanocrystals, and single-crystalline MnOOH nanowires is designed for the supercapacitor application, which is prepared by a simple two-step electrochemical deposition process. Because of the gradual co-transformation of Mn_3O_4 nanocrystals and a-MnO_2 nanorods into an amorphous manganese oxide, the cycle stability of a-MnO_2 is obviously enhanced by adding Mn_3O_4. This unique ternary oxide nanocomposite with 100-cycle CV activation exhibits excellent capacitive performances, i.e., excellent reversibility, high specific capacitances (470 F g^{-1} in $CaCl_2$), high power property, and outstanding cycle stability. The highly porous microstructures of this composite before and after the 10,000-cycle CV test are examined by means of scanning electron microscopy (SEM) and transmission electron microscopy (TEM).

1. Introduction

Due to the fact that supercapacitors cover a broad region on the power against energy density plane [1,2], this kind of devices are widely recognized as complementary charge storage assistance to rechargeable batteries in various applications which require transient but high/peak power pulses for the time-dependent usage [3]. Supercapacitors become a more and more important device in various stop-and-go systems (e.g., heavy hybrid vehicles, mass rapid transit, elevators, etc.), because supercapacitors with much lower equivalent series resistance (ESR) can capture and store pulse energy during the braking process, leading to much higher energy efficiency [3,4].

According to the charge storage mechanism, supercapacitors are generally divided into electrical double layer capacitors (EDLCs) using electrostatic charge separation and pseudocapacitors employing fast superficial redox reactions [1,2,4]. In comparing with EDLCs, higher capacitance can be achieved by using redox-active materials and crystalline ruthenium dioxide (RuO_2) in the hydrous form has been widely recognized as the best electrode materials for pseudocapacitors because of its high specific capacitance, good electronic conductivity, and cycle stability [5,6]. However, other transition metal oxides, such as MnO_2 [7], CoO_x [8], VO_x [9], Fe_3O_4 [10], and Ni–Co oxides [11,12] are recommended to replace RuO_2 because of their cost effectiveness. Among these candidates, MnO_2 seems to be the most promising material because of its excellent reversibility and acceptable specific capacitance [7,13]. This idea is further supported by the cycle stability improvement of amorphous MnO_2 (a-MnO_2) using suitable anions (e.g., HPO_4^{2-} or HCO_3^-) into the electrolyte [14].

In developing pseudocapacitive materials, relationships between the nanostructured architecture and the capacitive performances of active materials are widely investigated and discussed [2,5,12] because capacitance decreased rapidly in the high-rate applications due to depletion and over-saturation of working ions in the electrolyte [15,16] or significant potential drop of electron-hopping [17] during charge–discharge cycling. Based on these studies, fine-tuning the microstructures of electrode materials (e.g., nanowire and nanotube arrays) is believed to gain optimal performances in terms of energy density, power capability, and cycle stability. Hence, composites consisting of pseudocapacitive materials and porous carbon materials of various forms (e.g., activated carbon, mesoporous carbons, and carbon nanotubes) are commonly employed [18,19]. Unfortunately, the introduction of carbon-based skeleton usually reduces the total specific capacitance of composites and increases the complexity of electrode preparation [19]. Therefore, how to design and facilely establish an ideal microstructure of pseudocapacitor electrodes for efficiently enhancing the utilization and cycle stability of electroactive materials is still a challenge. In this work, a

* Corresponding author at: Department of Chemical Engineering, National Tsing Hua University, 101, Section 2, Kuang-Fu Road, Hsin-Chu 30013, Taiwan.
Tel.: +886 3 573 6027; fax: +886 3 573 6027.
E-mail address: cchu@che.nthu.edu.tw (C.-C. Hu).

0378-7753/$ – see front matter © 2010 Elsevier B.V. All rights reserved.
doi:10.1016/j.jpowsour.2010.08.001

hierarchical nanocomposite consisting of ternary manganese oxides, a-MnO_2, Mn_3O_4 nanocrystals, and MnOOH nanowires is designed to improve Mn oxide utilization and to improve the cycle stability of a-MnO_2.

2. Experimental

The wire-like Mn_3O_4/MnOOH nanocomposites were pulse-deposited onto graphite substrates from a deposition bath containing 0.1 M $Mn(CH_3COO)_2{\cdot}4H_2O$. The pretreatment of graphite substrates completely followed our previous work [20]. The exposed geometric area of substrates for deposition is 1 cm^2. Deposition was carried out in a two-electrode cell with a graphite cathode of the same size. The wave signals of pulse-rest plating were performed by means of a commercial power system (Jiehan 2050, Jiehan Inc., Taiwan). The total pulse electroplating time for Mn_3O_4/MnOOH deposits was 20 min. Amorphous MnO_2 was deposited at 4.0 mA cm^{-2} with a passed charge density of 0.2 C cm^{-2}. All solutions used in this work were prepared with pure water produced by a reagent water system (Milli-Q SP, Japan) at 18 MΩ cm. All reagents without further purification are Merck, GR. Solution temperature was maintained at 25 °C with an accuracy of 0.1 °C by means of a water thermostat (Haake DC3 and K20).

Cyclic voltammetry (CHI660C, CH Instruments Inc.) was conducted under a three-electrode mode in a solution of 0.5 M Na_2SO_4 or $CaCl_2$. The reference electrode and counter electrode were Ag/AgCl and platinum, respectively. The surface morphologies were examined by a field-emission scanning electron microscope (FE-SEM, Hitachi S4800-type I). The microstructures were observed through a field-emission transmission electron microscope (FE-TEM, FEI E.O Tecnai F20 G2).

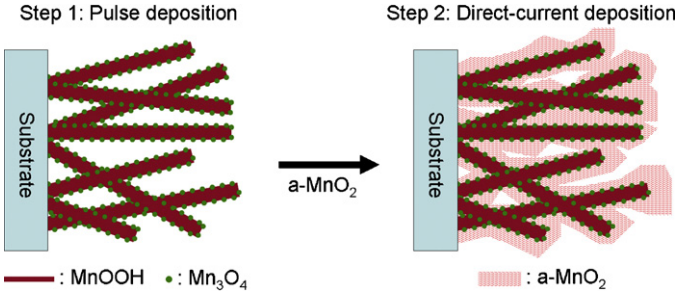

Fig. 1. The scheme for preparing hierarchical ternary manganese oxide composites: (step 1) pulse deposition of an Mn oxide deposit consisting of MnOOH nanowires and Mn_3O_4 nanocrystallites and (step 2) direct-current deposition of a-MnO_2 nanorods onto Mn_3O_4/MnOOH.

3. Results and discussion

The hierarchical nanocomposite consisting of a-MnO_2, Mn_3O_4 nanocrystals, and MnOOH nanowires is schematically shown in Fig. 1, which can be simply realized by a two-step electrochemical deposition since a two-electrode pulse-rest deposition mode was successfully developed to prepare a highly porous, wire-like nanostructure mainly consisting of MnOOH nanowires and Mn_3O_4 nanoparticles (step 1) [20]. In addition, the wire-like Mn_3O_4/MnOOH nanocomposite was found to be free-standing on various conductive substrates. Then, nanostructured a-MnO_2 with relatively high specific capacitance can be deposited onto the wire-like Mn_3O_4/MnOOH skeleton from the same deposition solution (step 2) [7,21]. The ternary manganese oxides with the designed nanostructure will show high utilization and long cycle stability of Mn oxides as well as facile preparation of electrodes. Note that

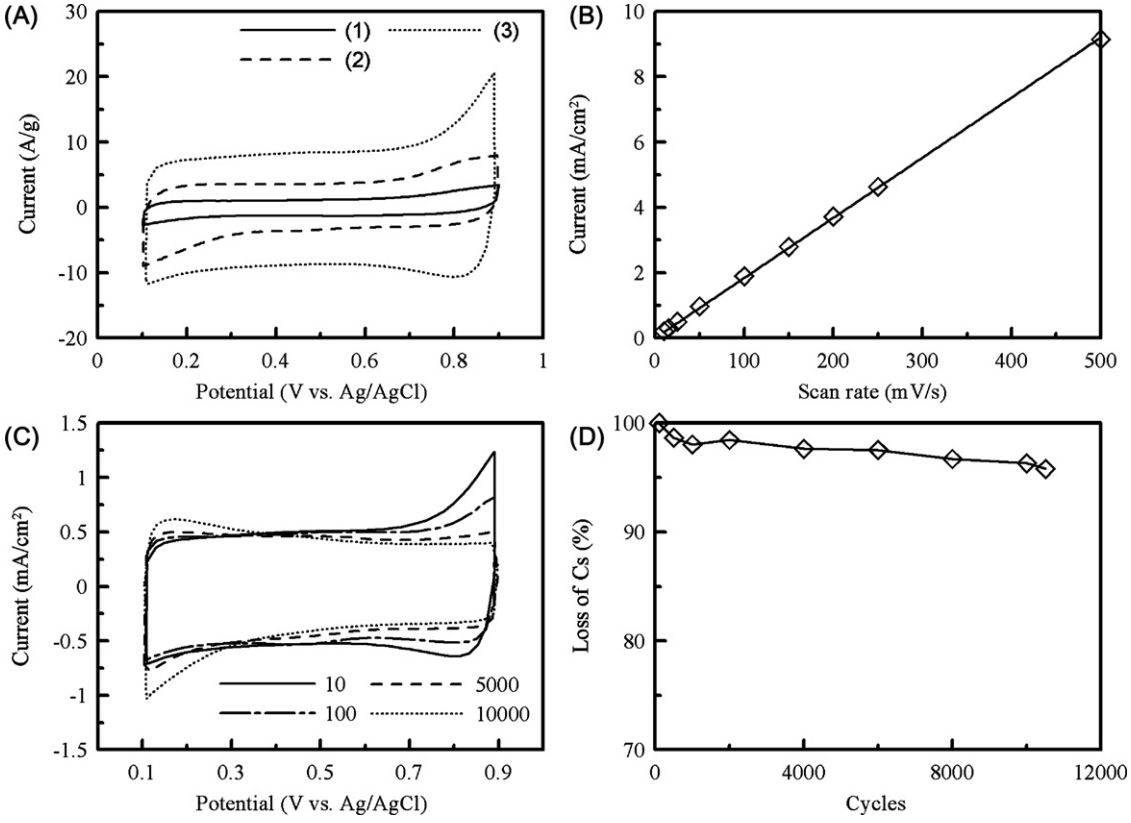

Fig. 2. (A) Cyclic voltammograms of (1) Mn_3O_4/MnOOH nanocomposite, (2) a-MnO_2 and (3) ternary a-MnO_2/Mn_3O_4/MnOOH nanocomposite in 0.5 M Na_2SO_4; (B) the quasi-linear dependence of capacitive current density measured at 0.5 V on the scan rate of CV, (C) cyclic voltammograms against cycle number and (D) specific capacitance retention against cycle number for an a-MnO_2/Mn_3O_4/MnOOH nanocomposite.

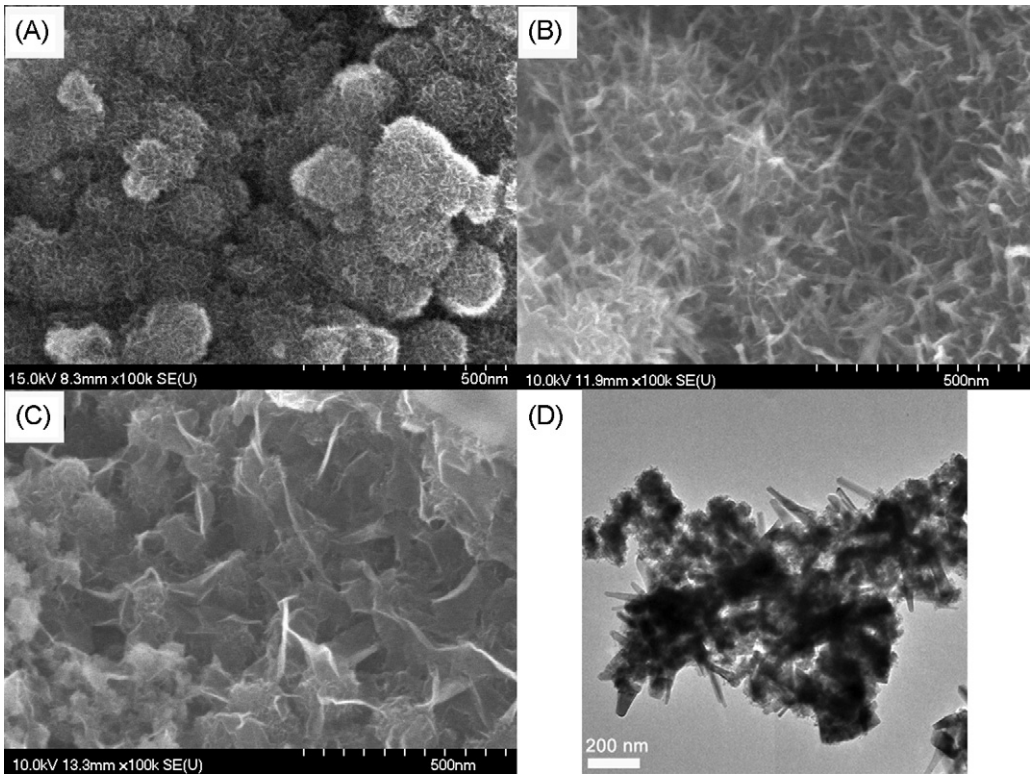

Fig. 3. (A–C) FE-SEM and (D) TEM images of (A) an as-prepared a-MnO_2/Mn_3O_4/MnOOH nanocomposite with (B) 1000, and (C and D) 10,000 cycles of CV in 0.5 M Na_2SO_4.

the resultant morphology, the length of MnOOH nanowires, and the relatively amount of Mn_3O_4 nanocrystals can be controlled by varying the pulse deposition variables [20], providing the merit for fine-tuning the architectures of porous MnOOH/Mn_3O_4 skeleton. In addition, the amount of a-MnO_2 has been demonstrated to simply control by the passed charge density [7,21], further emphasizing the merits of this hierarchical architecture design.

The excellent capacitive performances, i.e., good electrochemical reversibility, very high power property, and long cycle life, of the ternary manganese oxide nanocomposites are clearly demonstrated in Fig. 2. From a comparison of all curves in Fig. 2A, three features have to be mentioned. First, a-MnO_2, Mn_3O_4/MnOOH, and a-MnO_2/Mn_3O_4/MnOOH show capacitive-like behavior and fairly good electrochemical reversibility in the potential region of investigation. Second, the order of oxides with respect to decreasing the capacitive current density is: a-MnO_2/Mn_3O_4/MnOOH > a-MnO_2 > Mn_3O_4/MnOOH. Third, the sum of current density of curves 1 and 2 is significantly smaller than the current density of curve 3 although the specific capacitance of Mn oxides usually decreases with increasing the oxide loading [22]. The above results reveal the presence of a synergistic effect in constructing the ternary hierarchical architecture. Consequently, the specific capacitance (ca. 391 $F g^{-1}$) of the unique ternary a-MnO_2/Mn_3O_4/MnOOH nanocomposite is relatively high, revealing good utilization of Mn oxides. The high-rate capacitive performance is demonstrated by the quasi-linear dependence of the capacitive current density on the scan rate of CV (up to 500 $mV s^{-1}$) in Fig. 2B. This merit is ascribed to the highly porous, wire-like Mn_3O_4/MnOOH skeleton. In Fig. 2C, all CV curves are highly symmetric while the shape of cyclic voltammograms appears to gradually change with the 10,000-cycle test. The latter result is probably due to the simultaneous dissolution/transformation of a-MnO_2 and Mn_3O_4 into amorphous manganese oxide without any well-defined structure (see below). Fig. 2D reveals the long cycle stability of this ternary nanocomposite since the capacitive loss after 10,000 charge/discharge cycles between 0.1 and 0.9 V at 25 $mV s^{-1}$ is only 4.3% (based on the maximum specific capacitance value obtained after 100-cycle CV activation). The above results demonstrate the promising application potential of this ternary a-MnO_2/Mn_3O_4/MnOOH nanocomposite to supercapacitors.

From our previous work [20], the morphologies, such as nanowires and nanorods, of a-MnO_2 have been found to strongly depend on the deposition mode and deposition parameter, which should be also influenced by the cycling treatment. This statement is supported by our unpublished results that the surface morphology of Mn_3O_4 is gradually changed from a polyhedral structure into a sheet-like morphology in a 2000-cycle test. Accordingly, the resultant morphologies of the as-prepared a-MnO_2/Mn_3O_4/MnOOH nanocomposite and those with 1000 and 10,000 cycles of charge/discharge are compared and typical results are shown in Fig. 3. In Fig. 3A, the surface of pulse-plated Mn_3O_4/MnOOH deposit is covered with a layer of short and tiny a-MnO_2 nanorods, leading to a highly porous microstructure of the as-prepared nanocomposite. From a comparison of Fig. 3A–C, short and tiny a-MnO_2 nanorods are transformed into relatively long wires after the 1000-cycle test, which is transformed to a palmate-like morphology (i.e., sheet-like manganese oxide dispersed on MnOOH nanowires) after the 10,000-cycle test. The above change in surface morphologies should be simultaneously contributed by the dissolution/transformation of a-MnO_2 and Mn_3O_4, resulting in a better cycle stability in comparison with pure a-MnO_2 prepared by anodic deposition. The TEM image of this cycled nanocomposite in Fig. 3D clearly shows the morphology that nanowires were surrounded with numerous nano-sheets/aggregates which have been confirmed to be amorphous by selected area electron diffraction (not shown here). The nanowires in the cycled nanocomposite have also been confirmed to be MnOOH formed during the pulse deposition, which is very stable in the cycling test. The above results indicate that Mn_3O_4 nanocrystals and a-MnO_2 nanorods are gradually transformed into the amorphous manganese oxide during the

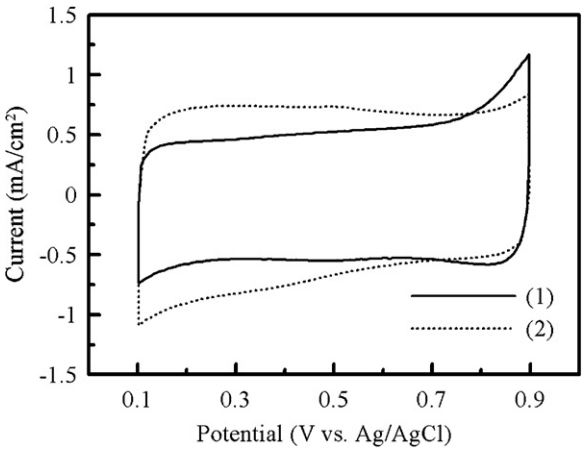

Fig. 4. Cyclic voltammograms measured in (1) 0.5 M Na_2SO_4 and (2) 0.5 M $CaCl_2$ for a ternary nanocomposite after the 10,000-cycle charge/discharge test.

cycling test and that Mn_3O_4 nanocrystals advance the cycle stability of *a*-MnO_2 prepared by electrodeposition.

Fig. 4 shows that the capacitive current density between 0.1 and 0.7 V for a ternary nanocomposite after the 10,000-cycle test is significantly promoted when the electrolyte is changed from Na_2SO_4 to $CaCl_2$ [23]. The specific capacitance is increased from 376.3 to 469.5 F g^{-1} (ca. 25% enhancement). Since the capacitance enhancement is below 10% for an as-prepared *a*-MnO_2/Mn_3O_4/MnOOH nanocomposite, the amorphous structure co-transformed from Mn_3O_4 nanocrystals and *a*-MnO_2 nanorods in the cycling test should be favorable for the charge storage/delivery in $CaCl_2$ although certain manganese oxides did not show such enhancement [24]. The exact reasons responsible for the above phenomena are under study.

4. Conclusions

The wire-like Mn_3O_4/MnOOH deposit prepared by pulse deposition is an ideal substrate for constructing a highly porous ternary *a*-MnO_2/Mn_3O_4/MnOOH nanocomposite. The cycle stability of *a*-MnO_2 is obviously enhanced by adding Mn_3O_4 due to the gradual co-transformation of Mn_3O_4 nanocrystals and *a*-MnO_2 nanorods into an amorphous manganese oxide. The completely symmetric *i*–*E* responses, the high specific capacitance (ca. 470 F g^{-1}), the high-power capacitive performance, and the long cycle stability of this ternary nanocomposite demonstrate the ideal architecture consisting of *a*-MnO_2, Mn_3O_4 nanocrystals, and MnOOH nanowires for improving Mn oxide utilization and depressing *a*-MnO_2 degradation in the supercapacitor application.

Acknowledgments

The financial support of this work, by the National Science Council of ROC, Taiwan under contract no. NSC 98-3114-E-007-011 and the boost program of NTHU, is gratefully acknowledged.

References

[1] R. Kötz, M. Carlen, Electrochim. Acta 45 (2000) 2483.
[2] J.W. Long, B. Dunn, D.R. Rolison, H.S. White, Chem. Rev. 104 (2004) 4463.
[3] J.R. Miller, A.F. Burke, ECS Interface Spring (2008) 53.
[4] B.E. Conway, Electrochemical Supercapacitors—Scientific Fundamentals and Technological Applications, Kluwer Academic/Plenum, New York, 1999.
[5] C.C. Hu, K.H. Chang, M.C. Lin, Y.T. Wu, Nano Lett. 6 (2006) 2690.
[6] K.H. Chang, C.C. Hu, C.Y. Chou, Chem. Mater. 19 (2007) 2112.
[7] C.C. Hu, T.W. Tsou, Electrochem. Commun. 4 (2002) 105.
[8] C.C. Hu, T.Y. Hsu, Electrochim. Acta 53 (2008) 2386.
[9] C.C. Hu, C.M. Huang, K.H. Chang, J. Power Sources 185 (2008) 1594.
[10] S.Y. Wang, N.L. Wu, J. Appl. Electrochem. 33 (2003) 345.
[11] C.C. Hu, C.Y. Cheng, Electrochem. Solid-State Lett. 5 (2002) A43.
[12] T.Y. Wei, C.H. Chen, H.C. Chien, S.Y. Lu, C.C. Hu, Adv. Mater. 22 (2010) 347.
[13] M. Toupin, T. Brousse, D. Belanger, Chem. Mater. 16 (2004) 3184.
[14] S. Komaba, A. Ogata, T. Tsuchikawa, Electrochem. Commun. 10 (2008) 1435.
[15] H. Zhou, D. Li, M. Hibino, I. Honma, Angew. Chem. Int. Ed. 44 (2005) 797.
[16] K.M. Lin, K.H. Chang, C.C. Hu, Y.Y. Li, Electrochim. Acta 54 (2009) 4574.
[17] K.H. Chang, Y.T. Wu, C.C. Hu, in: V. Gupta (Ed.), Recent Advances in Supercapacitors, Transworld Research Network, Kerala, India, 2006, pp. 29–56, chap. 3.
[18] J.K. Chang, C.T. Lin, W.T. Tsai, Electrochem. Commun. 6 (2004) 666.
[19] H. Zhang, G. Cao, Z. Wang, Y. Yang, Z. Shi, Z. Gu, Nano Lett. 8 (2008) 2664.
[20] C.C. Hu, K.H. Chang, Y.T. Wu, C.Y. Hung, C.-C. Lin, Y.T. Tsai, Electrochem. Commun. 10 (2008) 1792.
[21] C.C. Hu, C.C. Wang, J. Electrochem. Soc. 150 (2003) A1079.
[22] J.K. Changa, C.H. Huanga, M.T. Lee, W.T. Tsai, M.J. Deng, I.W. Sun, Electrochim. Acta 54 (2009) 3278.
[23] C. Xu, H. Du, B. Li, F. Kang, Y. Zeng, J. Electrochem. Soc. 156 (2009) A73.
[24] S.L. Kuo, N.L. Wu, J. Electrochem. Soc. 153 (2006) A1317.